

Load Testing Application for Truss Bridge Design Verification: Live Load Testing

Osman Hag-Elsafi¹; Jonathan Kunin²; and Sreenivas Alampalli^{3,*}

Submitted: 15 October 2024 Accepted: 11 December 2024 Publication date: 10 January 2025

DOI: 10.70465/ber.v2i1.15

Abstract: This companion paper discusses the application of load testing techniques for the verification of bridge design under live loads. This truss bridge is atypical to conventional design, with the top chords of the main trusses, floor beams, and stringers designed to act composite with the concrete deck. Under load, in addition to axial forces, such a design creates secondary moments in the truss main members and complicates the analysis. This inspired the need for verification of the bridge design through instrumentation, monitoring, and load-testing program.

Comparing the members' actual service load axial forces and moments with those used in the design, it was concluded that axial forces were overestimated in the design by about 20 percent for service dead load and by about 25 percent for service live load. A similar comparison for moments indicated that service dead load moments were within 20 percent of those used in the design, and service live load moments were underestimated by about 55 percent. The above differences in service dead load can be attributed to the way the deck pours were accounted for in the design and the possibility of construction loads being on the structure during the deck pour monitoring. For service live load, these differences can be explained by possible discrepancies in estimating service live load from the test results and the fact that the analysis for service live load in the design was performed ignoring the contribution of the composite concrete deck. The adequacy of the structural design under actual axial forces and moments was confirmed by checking the AASHTO interaction equations for steel members under combined axial and bending loading conditions.

Author keywords: Load Testing; Bridge Evaluation; Bridge Analysis; Bridge Design; Nondestructive Testing; Structural Monitoring; High Performance Steel (HPS); Truss Bridge

Introduction

Instrumentation, strain monitoring, and load testing of a bridge in Tioga County, New York, are discussed in a companion paper¹ and this paper. The bridge instrumentation, deck pour monitoring, and dead load analysis were discussed in the companion paper. Load testing and live load analysis are the focus of this paper. For completeness, the paper also verifies the adequacy of the bridge structural design by considering both dead load and live load in the analysis.

The bridge described in these papers is a continuous steel structure with a lightweight concrete deck. The concrete deck was built composite with the stringers as well as the top chords of the trusses. The fact that the deck is composite with the top chords of the trusses generally introduces secondary moments in the truss members and complicates structural

behavior. Moments in the truss members are also influenced by the behavior of the bolted connections, acting as pinned, semirigid, or rigid.

The companion paper discussed dead load design and described the instrumentation of the main members of the truss structure and the monitoring of strains in those members during concrete deck pours.¹ The instrumentation plans included mounting vibrating wire gages on five downstream truss members to determine axial forces and moments in the members during the pours. The instrumented members included a top and a bottom chord, two diagonals, and a vertical.

The objective of this companion paper is the verification of the live load design. To investigate live load axial forces and moments, additional strain data was collected during a load test using trucks of known weights and configurations. The load test was conducted immediately after construction was completed and before the bridge was opened to traffic. Finite element (FE) analysis was performed to determine the forces and moments in the truss members due to the load test trucks. The FE analysis and test results were then proportioned to estimate actual service load forces and moments in the bridge members.

*Corresponding Author: Sreenivas Alampalli.

Email: sreenivas.alampalli@stantec.com

¹New York State Department of Transportation (NYSDOT), Albany, NY 12232 (formerly with)

²New York State Department of Transportation, Albany, NY, 12232

³Stantec, New York, NY, 10017

Discussion period open till six months from the publication date. Please submit separate discussion for each individual paper. This paper is a part of the Vol. 1 of the International Journal of Bridge Engineering, Management and Research (© BER), ISSN 3065-0569.

Background and objectives

Instrumentation, strain monitoring, and load testing of a bridge in Tioga County, New York, are discussed in this paper. The bridge replaced an old bridge and carries Route 96 (Court Street) over Route 17 and the Susquehanna River into the Village of Owego (Fig. 1). It has six spans (52, 65, 65, 65, 65, 52, and 39 m) for a total length of 338 m. It is about 14.45 m wide, including a 12.40 m center-to-center spacing between two supporting trusses and two 1.02-m cantilever overhangs. It carries three lanes of traffic: northbound, southbound, and turning lanes. It has an average annual daily traffic (AADT) of about 6000 vehicles at the time of the testing.²

The bridge is a continuous steel structure consisting of stringers, floor beams, upstream and downstream trusses, and a lightweight concrete deck. Some of the top and bottom chord members of the upstream and downstream trusses were made of High-Performance Steel (HPS). The concrete deck was built composite with the stringers as well as the top chords of the trusses. The fact that the deck is composite with the top chords of the trusses generally introduces secondary moments in the truss members and complicates structural behavior. Moments in the truss members are also influenced by the bolted connections, behaving as pinned, semirigid, or rigid.

This work was initiated to investigate axial forces and moments in the main truss members due to service deck

dead load and service live load and verify the bridge design for live loads. Five of the downstream truss members were instrumented with vibrating wire gages to record strains in those members during the first three deck pours and to collect additional data during a load test conducted after the bridge construction was completed. The instrumented members were located near the Pier 1 side of Span 2 on the downstream truss (Spans 1 and 2, respectively, are shown in Figs. 2 and 3, and Pier 1 is shown in both figures). The instrumented members were carefully selected to be representatives of the most stressed members of the continuous trusses.

For verification of live load design, the paper presents relationships between the design service loads axial forces and moments (based on FE analysis results), and the actual axial forces and moments (based on monitoring and load testing results) for the instrumented members.^{1,2}

Paper organization

The load test plans were first discussed, followed by the analysis of the strain data collected during the load testing. Test data were compared with the finite element analysis results. Actual service load axial forces and moments due to live load in the instrumented members were then estimated. A summary of the dead load and live load results is then given, and the adequacy of the bridge design is verified using those results. The paper closes with concluding remarks and



Figure 1. Court street bridge



Figure 2. Span 1 downstream view



Figure 3. Span 2 downstream view

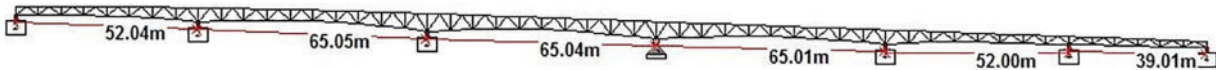


Figure 4. Two-dimensional bridge model

recommendations for the design of similar structures in the future.

Analysis and Design of the Bridge Structure

Bridge analysis

The bridge analysis and design were discussed in the companion paper (Hag-Elsafi, Kunin, and Alampalli 2024).¹ The STAAD III results were investigated using truss and frame analysis options, for both two- and three-dimensional models (Figs. 4 and 5). Axial live load forces in the bridge members were determined, mainly based on the BLRS program, using a truss model and an adjusted AASHTO HS-20 load to reflect an HS-25 line load. A two-dimensional STAAD III frame model, assuming the end fixity of the truss members, was loaded with combination lane loadings to produce maximum axial forces in chord members at midspan and at the piers (Fig. 4). The maximum stresses resulting from the BLRS and STAAD III analysis (2-dimensional models) were compared and the higher of the two stresses was used in the final design.

Secondary moments due to live load were calculated by applying an equivalent truck load along the two-dimensional truss model top chord as a moving load in two scenarios. The truck axle weights were proportioned to resemble that of an HS-25 (W/4, W, W), and a 3.25-m axle spacing was selected so that the axles would always coincide with the top chord nodal points. The axle weight W was calculated from the following equation:

$$W = (\text{HS} - 25 \text{ Axle Weight}) \times (\text{Live Load Distribution Factor}) \times (\text{Impact}) \times (\text{Lane Load Modifier}) \quad (1)$$

where HS-25 axle load = 178 kN, Live Load Distribution Factor = 1.68 trucks for downstream truss, impact = 1.15 (assumed average value for the bridge), and Lane Load Modifier = 1.27 (ratio of HS-25 lane load to truck load simple span moment for 65-m span, which was used to make the truck load approximate a lane load application). Substituting these values in the above equation, W can be obtained as 437 kN.

In the first scenario, the moving load was applied on a two-dimensional STAAD III model at 3.25-m increments

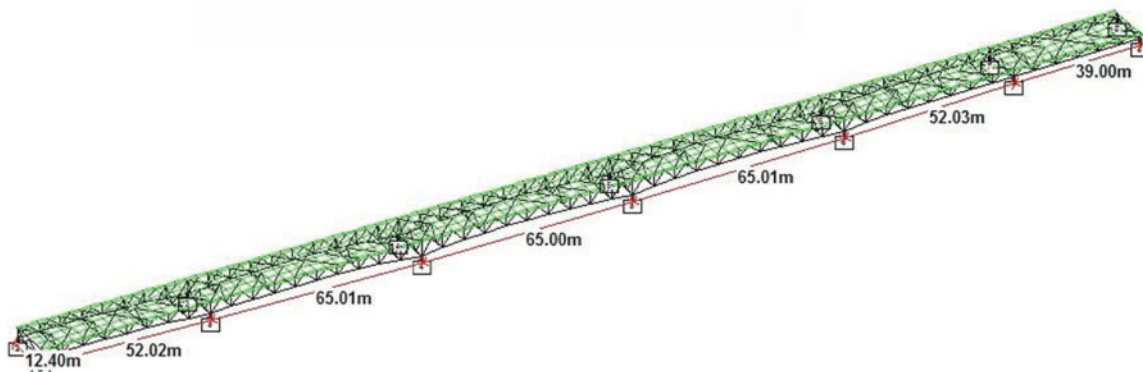


Figure 5. Three-dimensional bridge model

Table 1. Service load axial forces and moments

Gage number	Member mounted on	Service load axial forces and moments			
		Live load including impact		Dead load	
		Axial force (kN)	Secondary moment (kN-m)	Axial force (kN)	Secondary moment (kN-m)
1, 2	U16-L16	-400	5	-343	1
3, 4	L16-U17	-1318	28	-2291	38
5, 6, 7, 8	L16-L18	-2652	114	-5120	241
9, 10	U17-L18	1246	24	1931	22
11, 12	U16-U17	3281	224	6423	267

to coincide with top chord nodal points. Maximum positive and negative moments and maximum compression and tension axial forces in the members were recorded. In the second scenario, the moving load was applied on the two-dimensional STAAD III model at 0.825-m increments (3.25/4) to produce direct live load stringer moments in the top chord as well as secondary moments from truss node fixity. Only maximum moments were recorded from this analysis. Results from the above analyses were entered into a spreadsheet to determine design live load secondary moments. The axial forces and secondary moments based on the above analysis for the instrumented members are

summarized in Table 1. The members referenced in this table are defined in the Span 2 framing plan (see companion paper). A transverse section through the bridge showing the cross frames detail at Pier 1 and the composite concrete deck (with the stringers and the top chords) is also shown in the same figure.

Bridge design

The bridge was designed based on the New York State Department of Transportation Standard Specifications for Highway Bridges, with all provisions in effect during

Table 2. Members shape and steel grades

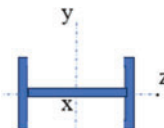
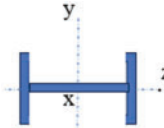
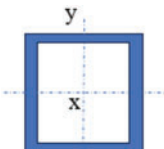
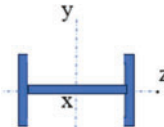
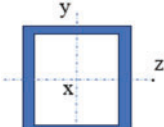
Gage number	Member mounted on	Section	Length (mm)		Thickness (mm)		Steel grade	F _y (MPa)
			Web	Flange	Web	Flange		
1	U16-L16		533	270	10	14	345 W	345
2	U16-L16							
3	L16-U17		533	433	14	30	345 W	345
4	L16-U17							
5	L16-L18		533	533	28	18	485 W	485
6	L16-L18							
7	L16-L18							
8	L16-L18							
9	U17-L18		533	473	10	28	345 W	345
10	U17-L18							
11	U16-U17		533	533	38	20	485 W	485
12	U16-U17							

Table 3. Instrumented members' properties

Member	Length (m)	Gross area (m ²)	$I_{zz} \cdot 10^{-3}$ (m ⁴)	$I_{yy} \cdot 10^{-3}$ (m ⁴)	$S_z \cdot 10^{-3}$ (m ³)	$S_y \cdot 10^{-3}$ (m ³)	$r_z \cdot 10^{-1}$ (m)	$r_y \cdot 10^{-3}$ (m)	L/r
U16-L16	4.00	0.0126	0.05	0.62	0.34	2.44	2.21	0.60	66.25
L16-U17	5.15	0.031	0.32	1.64	1.60	6.49	2.32	1.02	50.02
L16-L18	6.52	0.0470	1.61	2.22	7.16	8.79	2.26	1.92	33.82
U17-L18	4.88	0.0255	0.24	1.41	1.18	5.60	2.35	0.96	51.09
U16-U17	3.25	0.0588	2.16	2.80	8.10	12.6	2.26	1.86	17.46

the design,¹ including AASHTO Standard Specifications for Highway Bridges, 16th edition and interims, and the AASHTO Guide Specifications for Strength Design of Truss Bridges (Load Factor Design) and Interims.³⁻⁶

The bridge superstructure steel conforms to ASTM A709M Grade 345 W (non-HPS) or ASTM A709M Grade 485 W (HPS). An elastic modulus of 2×10^5 MPa was specified for the design of both steel-type members.⁷ The instrumented members' shapes, web, and flange dimensions, steel grades, and yield stresses (F_y) are shown in Table 2. The members' properties [moment of inertia (I), section modulus (S), radius of gyration (r), and length (L) over radius of gyration ratio (L/r)] are given in Table 3. For design purposes, compressive strength, and elastic modulus of concrete for the substructure and deck slab at 28 days were also specified at 21 and 1.64×10^4 MPa.

Load Testing and Analysis

Load testing of the bridge was planned to provide data for the investigation of axial forces and secondary moments in the downstream truss members. The gages were mounted in pairs near members' ends to collect strain and temperature data during the first three deck pours and for a post-construction load test. Vibrating wire gages (Geokon Model 4000) were used for their long-term durability and did not require correction for drift. The gages were read using a Geokon Model GK-403 Readout Box, which reads one gage at a time, giving the gage's strain in $\mu\epsilon$ and temperature in °C. The vibrating wire gages have a Gage Correction Factor of 0.945.

Load test plans

The test plans included loading the bridge with four trucks (Trucks I, II, III, and IV) of known weights and configurations to maximize forces and moments at the gage

**Figure 6.** Three and four-axle load test trucks**Table 4.** Test trucks weight data

Truck	Front axle weights (kN)		Back axle weights (kN)		Truck gross weight (kN)
	Left side tires	Right side tires	Left side tires	Right side tires	
I	42.3	35.5	97.9	100.1	275.8
II	42.3	48.9	93.2	89.2	273.6
III	42.3	44.5	104.5	91.2	282.5
IV	44.5	42.3	124.5	109.0	320.3

locations near Pier 1. All the trucks had 3 axles, except for Truck I, which had four axles (Fig. 6). Axle weights and configurations for the four trucks are given in Table 4. To simplify the analysis, each truck in this table was reduced to a two-axle configuration by representing the rear axle left and right tire weights by single loads. Four loading formations (Load Cases A, B, C, and D) were selected to place the trucks on the bridge deck at the positions shown in Fig. 7. These positions were determined, as practically as possible, to maximize the instrumented member forces and moments. Transversely, the trucks were positioned as close as possible to the downstream curb to maximize the load on the downstream truss. Photos taken during the testing for Load Cases C and D are shown in Figs. 8 and 9, respectively. As seen in Fig. 7, Load Cases A and B were like Load Cases D and C, respectively. However, the truck locations along the

bridge were different for the respective cases. Fig. 10 shows Trucks I and II positions in Load Cases B and C formations.

Load test results

Besides deck-monitoring strains, additional strains were collected during the four load test cases. Because the tests were conducted in a relatively short period of time, changes in temperature were minimal and did not warrant correcting the data for temperature effects. Recorded strain data at the various gages was used to calculate the stresses in Table 5 for all load cases.

The three-dimensional STAAD III model was loaded in a manner replicating the actual truck loads on the bridge during the load test to obtain FE results for axial forces and moments. Utilizing these results together with the properties in Tables 2 and 3, and gage locations in Table 6, member

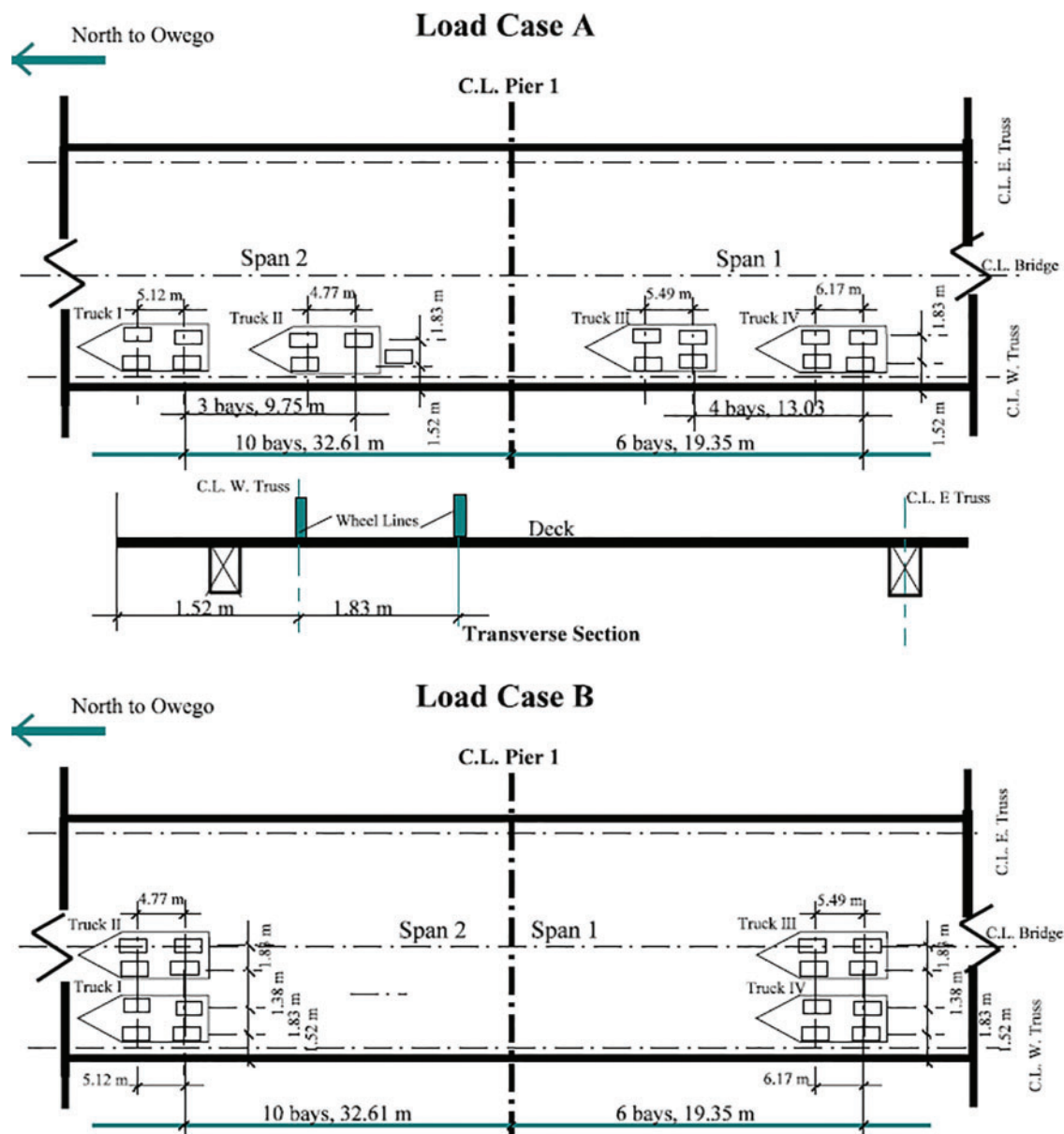


Figure 7. (Continued)

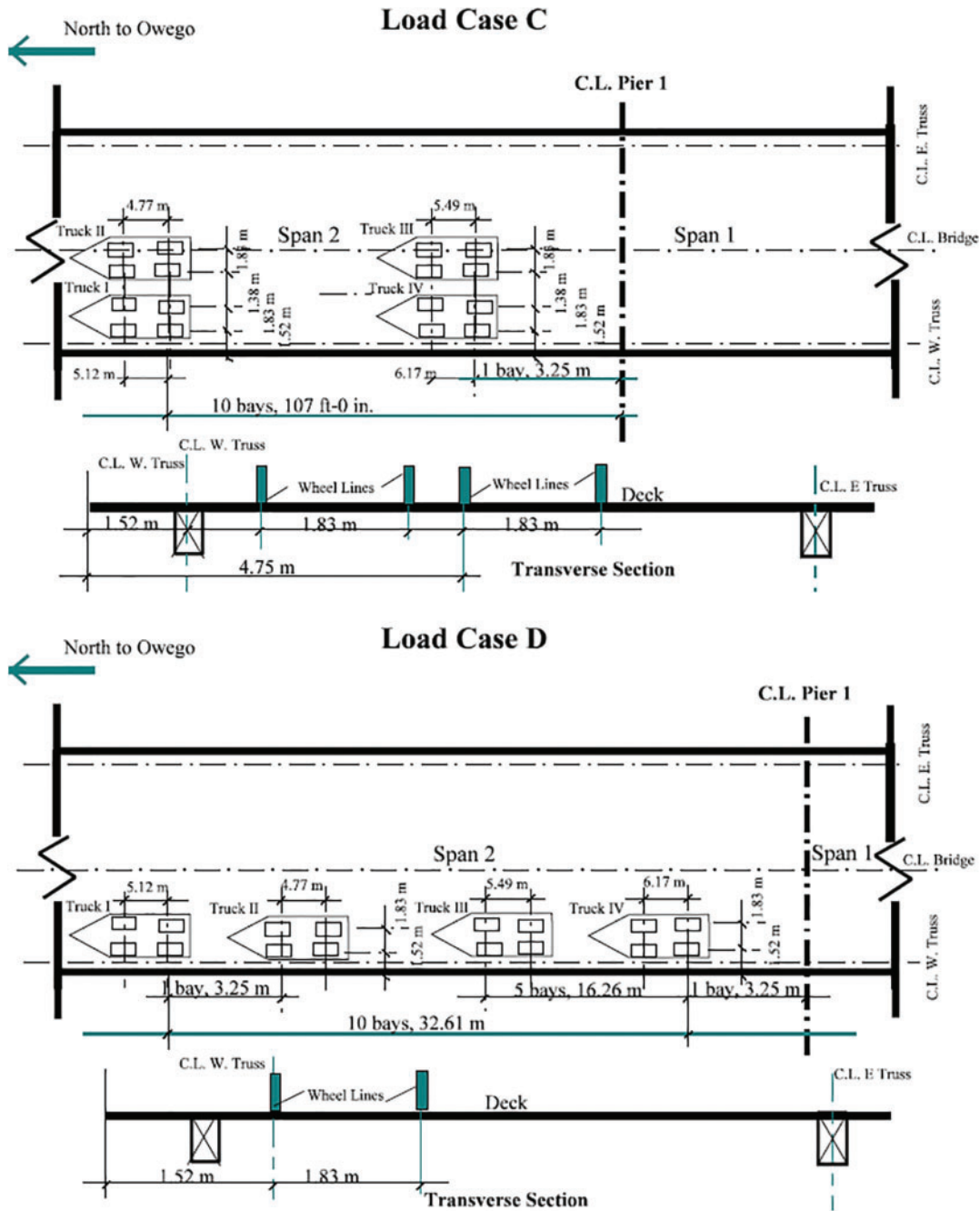


Figure 7. Load test truck locations on the bridge

stresses at gage locations can be determined as shown in Table 7.

As mentioned in the previous section, measured stress at a gage location is the net contribution of the individual stress components at that location. The stress components for the test results in Table 7 were determined by solving the two stress equations for each paired gage on a member for the z-axis bending stress and then using a pseudo-analytical approach to determine the axial and y-axis bending stresses, as illustrated below.

Gages 7 and 8 stresses will be used for this illustration. From Fig. 11, The following stress equations can be written at the two gage locations on Member L16–L18:

$$\sigma_A + \sigma_y + \sigma_z = \text{Gage 7 Stress} \quad (2)$$

$$\sigma_A + \sigma_y - \sigma_z = \text{Gage 8 Stress} \quad (3)$$

where σ_A , σ_y , and σ_z , respectively, are the stresses due to axial forces, bending about the y-axis, and bending about the z-axis-. Solving the above equations for σ_z :

$$\sigma_z = (\text{Gage 7 Stress} - \text{Gage 8 Stress})/2 \quad (4)$$

Adding Eqs. (2) and (3), and solving for σ_A :

$$\sigma_A = (\text{Gage 7 Stress} + \text{Gage 8 Stress})/[2(1 + R)] \quad (5)$$

where $R = \sigma_y/\sigma_A$. This ratio is determined from the finite element results in Table 7. Once σ_z and σ_A are determined



Figure 8. Trucks for load case C formation



Figure 9. Trucks for load case D formation



Figure 10. Trucks I and II for load cases B and C formations

from Eqs. (4) and (5), respectively, and σ_y can be obtained from either Eqs. (2) or (3).

The load test and FE stress results for the four load cases are compared in Table 8 and Fig. 12. From these results, it can be concluded that the FE and test stress results compare

very well and that the FE stresses are generally higher than the test stresses for all gages, except for those mounted on Member U16-L16 (Gages 1 and 2).

Live load analysis

The objective of this section is to determine actual axial forces and secondary moments in the instrumented members under service live load. This would require comparing/proportioning the load test effects (moment and shear) to those due to the service live load used in the members' design. For that, a one-dimensional model of the downstream truss was loaded with the service load combinations producing maximum moment and shear at the gage locations (Fig. 13) and also with the equivalent axle loads on the truss during the four load test cases (Fig. 14). The moment and shear results from this analysis, at Pier 1 end of Span 2, are summarized in Table 9. The table shows load test moments and shear forces expressed as percentages of the maximum moments and shear forces due to the governing service load combinations. For each load case, an average percentage of its moment and shear is assumed to give the percentage the load case represents of the design service live load moment and shear. From Table 9, those were obtained as 34, 29, 43, and 54 percent for Load Cases A, B, C, and D, respectively.

Using the stress data in Table 7, the properties in Table 3, and applying the appropriate percentages from Table 9, the relationship between the design service load and test loads axial forces and moments can be established as shown in Table 10, and Figs. 15–17. From these figures, the actual service load axial force/moment can be determined on the horizontal axis for any member's axial force/moment design service load force/moment on the vertical axis. Note that the linear relationships between the test and FE results in the figures prove the consistency of the load test data and the linear performance of the structure. Data points located off the best-fit lines in the figures correspond to load cases producing more eccentric loading (Load Cases B and C). From Fig. 15, it can be concluded that actual service load axial forces are about 20 percent lower than those used for the members' design. In Table 10, the three-dimensional FE analysis was able to detect a behavior that could not have been detected by two-dimensional analysis: the presence of significant out-of-plane bending (bending about the y-axis) under some loading scenarios. This emphasizes the importance of three-dimensional analysis in investigating the structural behavior of a bridge of this type.

Analyses of the data sets used to generate Figs. 15–17 can be found in Appendix D of Hag-Elsafi, Kunin, and Alampalli 2006² and show the statistical significance of the relationships between FE and test results established in these figures.

The goal in this section is to determine axial forces and secondary moments in the instrumented members under total service dead load, using the service deck load analysis results, and are presented in Figs. 18 and 19. These show a good correlation as seen from these figures.

Table 5. Stresses for the load test cases

Gage number	Member mounted on	Gage stress (MPa)			
		Load case			
		A	B	C	D
1	U16-L16	-6.44	-2.55	-14.59	-9.83
2	U16-L16	-7.33	-4.48	-15.99	-9.54
3	L16-U17	-5.36	-2.23	-17.64	-19.87
4	L16-U17	-12.41	-11.80	-16.06	-17.54
5	L16-L18	-16.81	-15.96	-6.76	-11.02
6	L16-L18	-15.67	-15.60	-3.69	-6.02
7	L16-L18	-15.64	-15.90	-2.88	-6.27
8	L16-L18	-17.98	-16.03	-10.15	-17.43
9	U17-L18	9.10	7.82	3.36	9.34
10	U17-L18	5.91	4.00	8.55	14.36

Table 6. Gage locations on members

Gage number	Member mounted on	Distance from starting member's end (m)
1	U16-L16	1.41
2	U16-L16	1.41
3	L16-U17	1.58
4	L16-U17	1.58
5	L16-L18	5.30
6	L16-L18	5.30
7	L16-L18	1.64
8	L16-L18	1.64
9	U17-L18	1.46
10	U17-L18	1.46
11	U16-U17	1.35
12	U16-U17	1.35

Table 7. Stress components based on load tests and FE analysis

Load case	Member	Load case stresses (MPa)					
		Axial (σ_A)		z-axis bending (σ_z)		y-axis bending (σ_y)	
		FE	Test	FE	Test	FE	Test
A	U16-L16	-5.43	-6.02	-0.31	-0.44	-0.78	-0.86
	L16-U17	-9.97	-8.70	-1.49	-1.60	-0.46	-1.19
	L16-L18	-21.6	-15.58	-4.36	-1.17	-1.71	-1.23
	U17-L18	11.76	8.49	0.53	3.52	1.61	0.39
	L16-L18	-21.60	-16.11	-1.29	-0.57	-0.18	-0.13

Table 7. Continued

Load case	Member	Load case stresses (MPa)					
		Axial (σ_A)		z-axis bending (σ_z)		y-axis bending (σ_y)	
		FE	Test	FE	Test	FE	Test
B	U16-L16	-1.36	-3.31	-0.25	-0.96	-0.08	-0.19
	L16-U17	-7.32	-6.98	-1.21	-4.79	-0.04	-0.04
	L16-L18	-22.71	-15.82	-3.80	-0.07	-0.22	-0.16
	U17-L18	8.60	6.12	0.67	1.91	0.30	0.21
	L16-L18	-22.71	-15.44	-1.53	-0.18	-0.50	-0.34
C	U16-L16	-8.31	-11.88	-0.83	-0.70	-2.39	-3.46
	L16-U17	-20.29	-15.68	-0.34	-0.79	-1.52	-1.18
	L16-L18	-7.17	-4.65	-2.96	-3.64	-2.88	-1.87
	U17-L18	16.12	9.67	2.13	2.59	6.19	3.71
	L16-L18	-7.17	-5.57	-1.21	-1.53	-0.44	-0.34
D	U16-L16	-4.70	-7.90	-1.00	-0.15	-1.00	-1.73
	L16-U17	-25.40	-17.92	-0.55	-1.77	-1.10	-0.76
	L16-L18	-12.76	-7.69	-4.33	-5.58	-6.91	-4.17
	U17-L18	24.00	16.00	2.10	2.51	6.30	4.20
	L16-L18	-12.76	-10.21	-0.64	-2.50	-2.11	-1.68

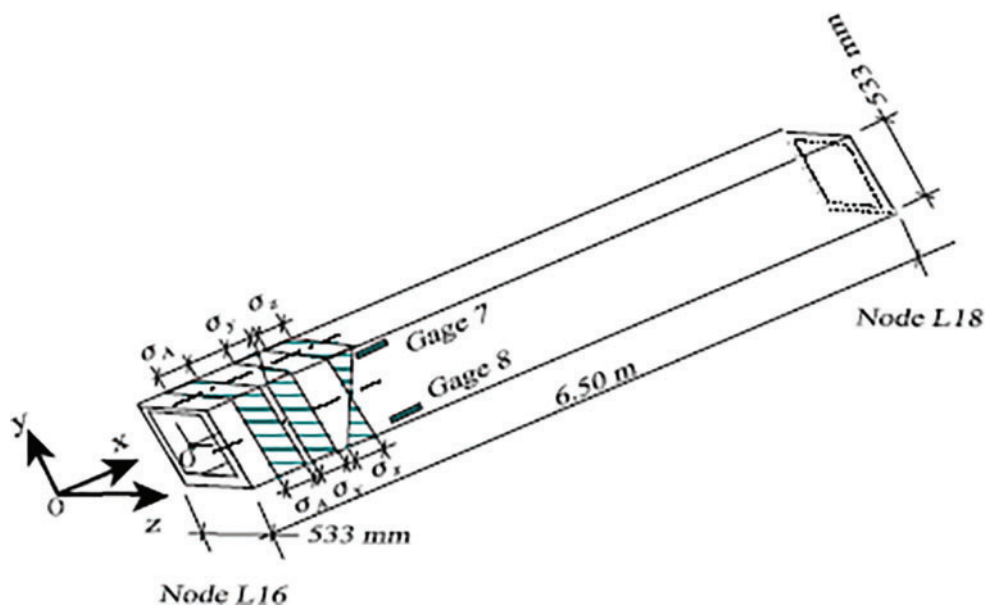


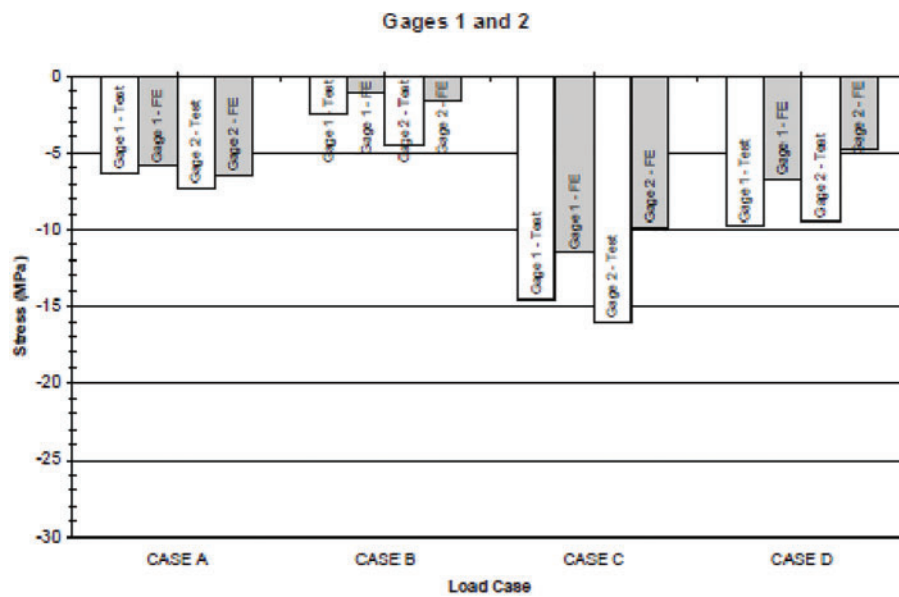
Figure 11. Member L16–L18 stresses

Table 8. Test versus FE stresses for the four load cases

Gage number	Member mounted on	Result type	Gage stress (MPa)			
			Load case			
			A	B	C	D
1	U16-L16	Test	-6.44	-2.55	-14.59	-9.83
		FE	-5.81	-1.18	-11.53	-6.75

Table 8. Continued

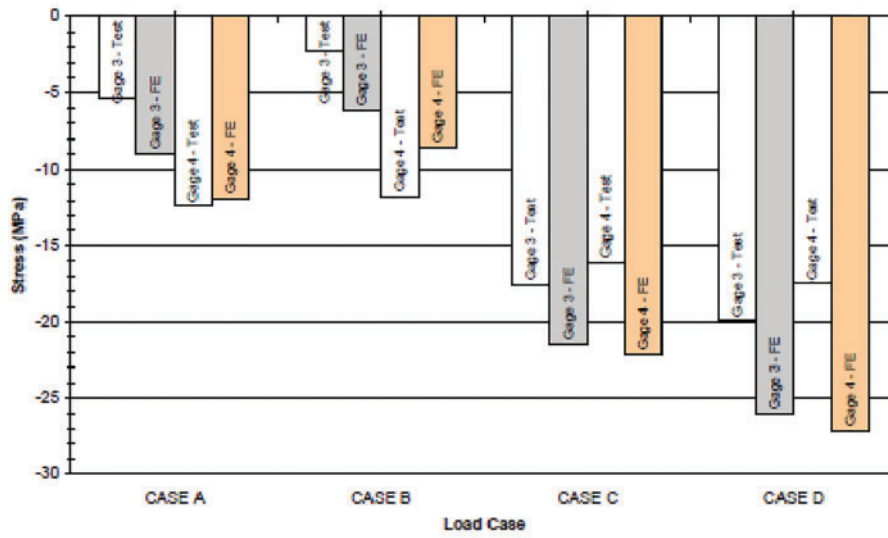
Gage number	Member mounted on	Result type	Gage stress (MPa)			
			Load case			
			A	B	C	D
2	U16-L16	Test	-7.33	-4.48	-15.99	-9.54
		FE	-6.51	-1.70	-9.87	-4.72
3	L16-U17	Test	-5.36	-2.23	-17.64	-19.87
		FE	-8.95	-6.15	-21.47	-25.99
4	L16-U17	Test	-12.41	-11.80	-16.06	-17.54
		FE	-11.91	-8.57	-22.15	-27.09
5	L16-L18	Test	-16.81	-15.96	-6.76	-11.02
		FE	-20.54	-21.69	-7.94	-11.29
6	L16-L18	Test	-15.67	-15.60	-3.69	-6.02
		FE	-23.12	-24.74	-5.52	-10.02
7	L16-L18	Test	-15.64	-15.90	-2.88	-6.27
		FE	-19.00	-19.14	-7.10	-15.34
8	L16-L18	Test	-17.98	-16.03	-10.15	-17.43
		FE	-27.71	-26.73	-13.01	-24.01
9	U17-L18	Test	9.10	7.82	3.36	9.34
		FE	10.67	9.02	7.80	15.49
10	U17-L18	Test	5.91	4.00	8.55	14.36
		FE	9.62	7.68	12.05	19.87



Member U16-L16

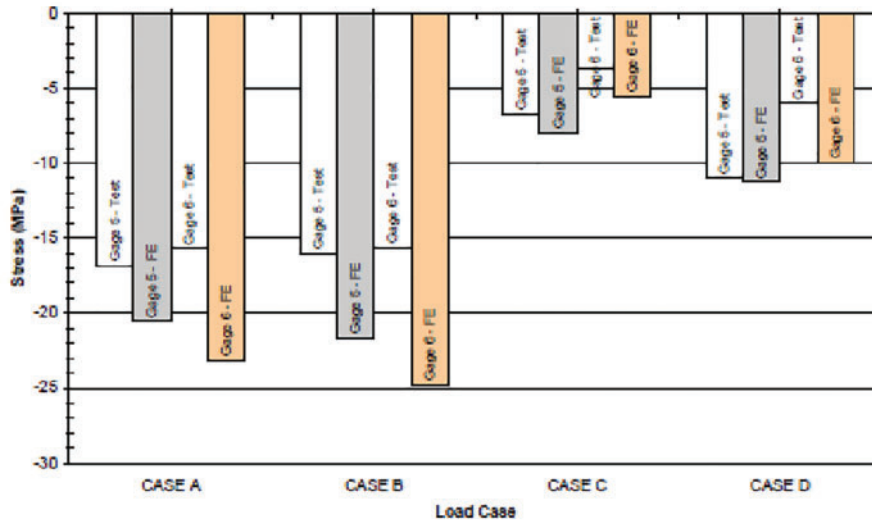
Figure 12. (Continued)

Gages 3 and 4



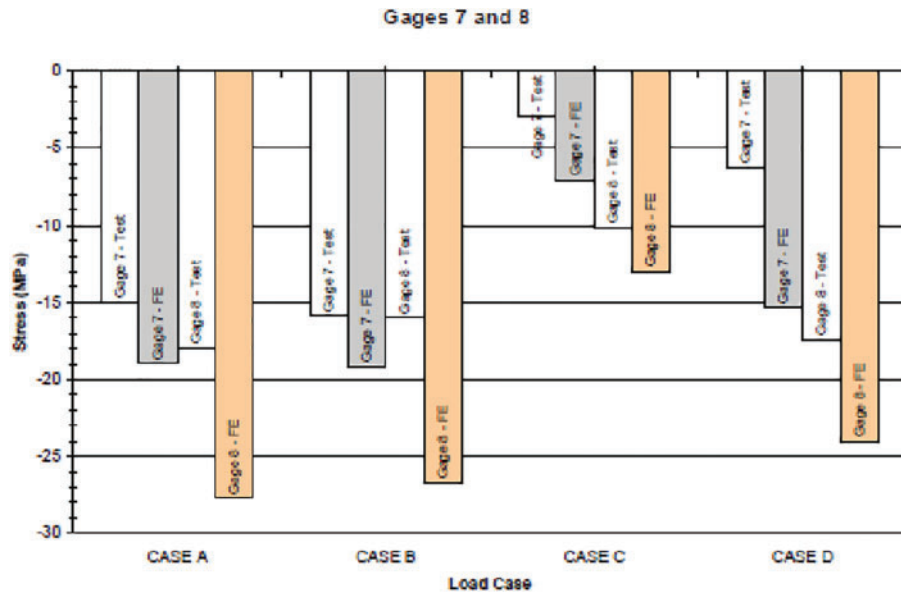
Member L16-U17

Gages 5 and 6

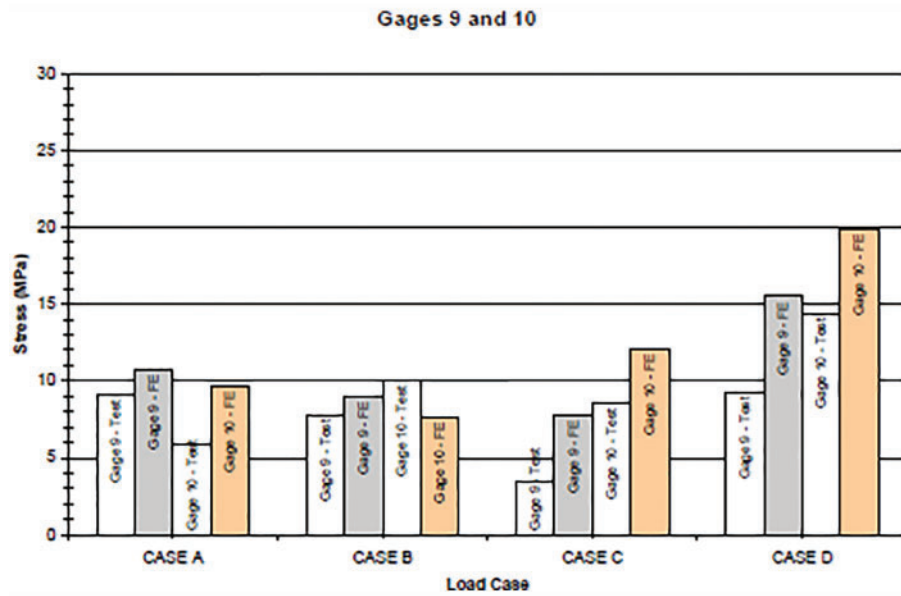


Member L16-L18

Figure 12. (Continued)



Member L16-L18

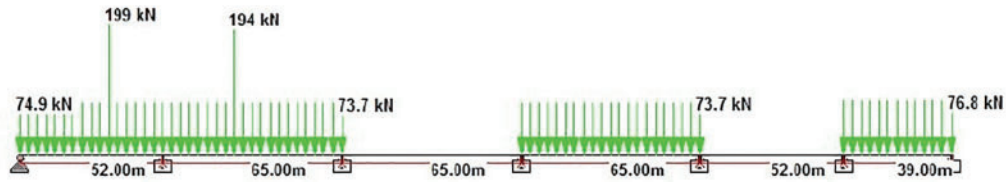


Member U17-L18

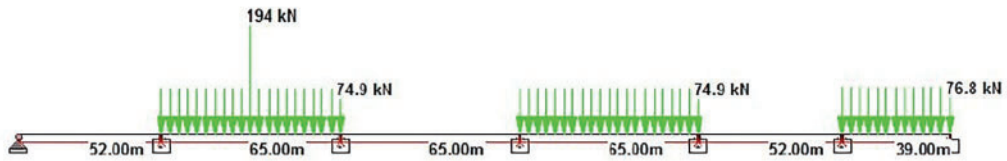
Figure 12. Comparison of test and FE stresses for the four load cases



Load Combination 134



Load Combination 139

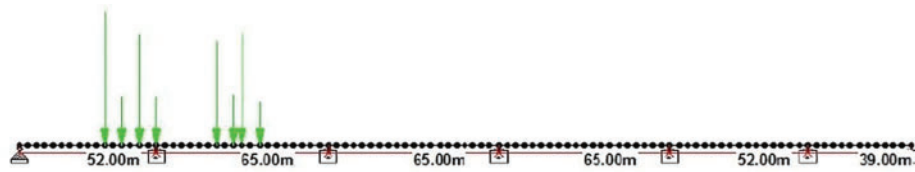


Load Combination 156

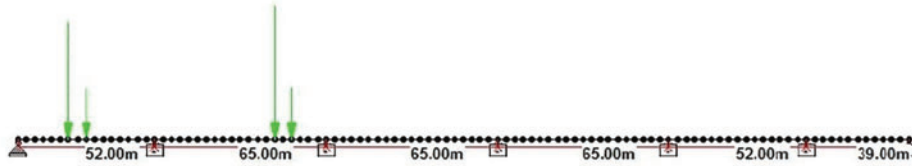


Load Combination 161

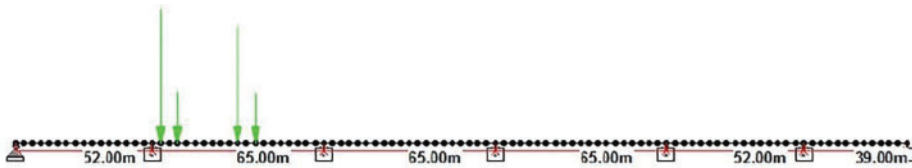
Figure 13. Governing service live load combinations for maximum moment and shear



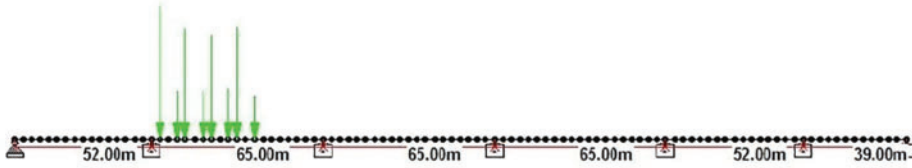
Load Case A (69, 175, 80, 164, 77, 174, 77, and 210 kN)



Load Case B (126, 292, 131, and 334 kN)



Load Case C (126, 292, 131, and 334 kN)



Load Case D (69, 175, 80, 164, 77, 174, 77, and 210 kN)

Figure 14. Axle loads on the downstream truss during the load tests (ordered right to left)

Table 9. Moment and shear results for service load combinations and load cases

Load case	Test		Design service load (From FE analysis)			Test to maximum design service load (%)		
	Moment and shear at gages locations on span 2		Load combination	Moment and shear at gages locations on span 2		Moment	Shear	Average
	Moment (kN-m)	Shear (kN)		Moment (kN-m)	Shear (kN)			
A	4393	306	134*	–	–	38.5	28.8	33.7
B	3200	317	139	11396	942	28.1	29.8	28.9
C	3150	633	156	6748	840	27.6	59.5	43.6
D	4476	743	161	10131	1063	39.3	69.9	54.6
	Maximum FE analysis			11396	1063			

Note: *Load Combination 134 produces negative bending in Span 2.

Table 10. Axial forces and moments: service live load (FE) versus load test

Load case	Gage number	Member mounted on	Axial force F_x (kN)		z-axis bending M_z (kN-m)		y-axis bending M_y (kN-m)	
			FE	Test	FE	Test	FE	Test
A	1, 2	U16-L16	-201.4	-223.3	-0.3	-0.4	-5.6	-6.2
	3, 4	L16-U17	-897.3	-783.0	-7.0	-7.5	-8.8	-22.7
	5, 6	L16-L18	-2985.9	-2227.0	-27.1	-12.0	-4.7	-3.3
	7, 8	L16-L18	-2985.9	-2153.7	-91.8	-24.6	-44.2	-31.8
	9, 10	U17-L18	882.0	636.8	1.8	12.2	26.5	6.4
B	1, 2	U16-L16	-59.1	-143.9	-0.3	-1.1	-0.7	-1.6
	3, 4	L16-U17	-772.4	-736.5	-6.7	-26.4	-0.9	-0.9
	5, 6	L16-L18	-3680.6	-2502.3	-37.7	-4.4	-15.3	-10.3
	7, 8	L16-L18	-3680.6	-2563.9	-93.8	-1.7	-6.6	-4.9
	9, 10	U17-L18	756.2	538.1	2.7	7.8	5.8	4.1
C	1, 2	U16-L16	-262.0	-374.5	-0.7	-0.6	-14.6	-21.1
	3, 4	L16-U17	-1552.2	-1199.5	-1.4	-3.2	-24.7	-19.2
	5, 6	L16-L18	-842.5	-654.5	-21.6	-27.4	-9.6	-7.5
	7, 8	L16-L18	-842.5	-546.4	-52.9	-65.1	-63.3	-41.1
	9, 10	U17-L18	1027.7	616.5	6.3	7.6	86.6	51.9
D	1, 2	U16-L16	-118.5	-199.2	-0.7	-0.1	-4.9	-8.5
	3, 4	L16-U17	-1554.5	-1096.7	-1.8	-5.7	-14.3	-9.9
	5, 6	L16-L18	-1199.5	-959.7	-9.1	-35.8	-37.1	-29.5
	7, 8	L16-L18	-1199.5	-722.9	-62.0	-79.9	-121.5	-73.3
	9, 10	U17-L18	1224.0	816.0	5.0	5.9	70.5	47.0

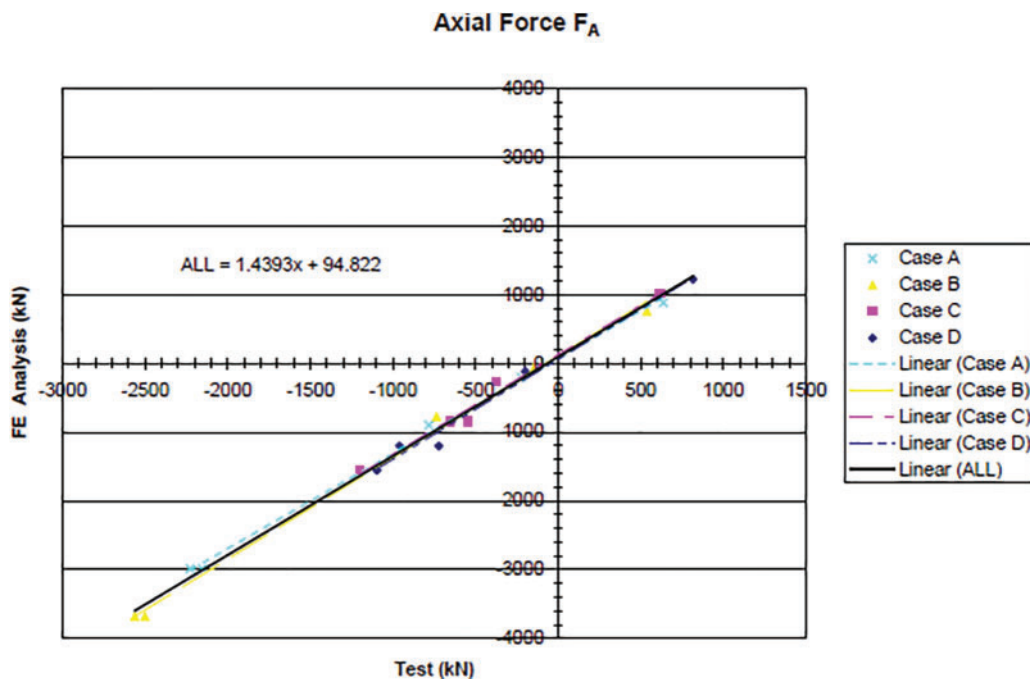


Figure 15. Axial force (F_A): service live load (FE Analysis) versus load test

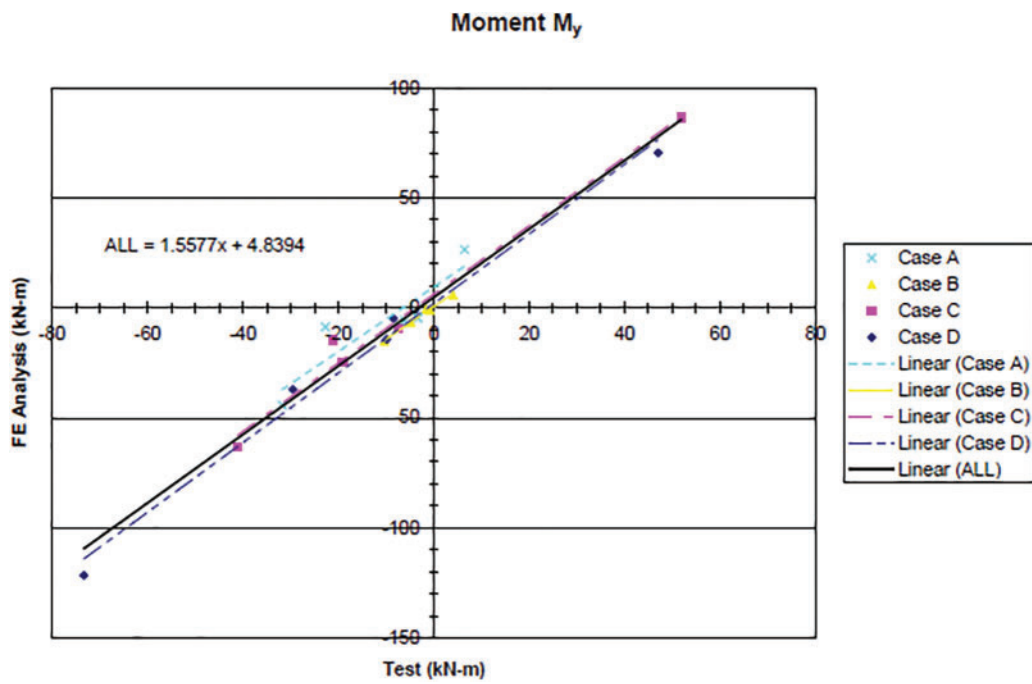


Figure 16. Bending moment (M_y): service live load (FE Analysis) versus load test

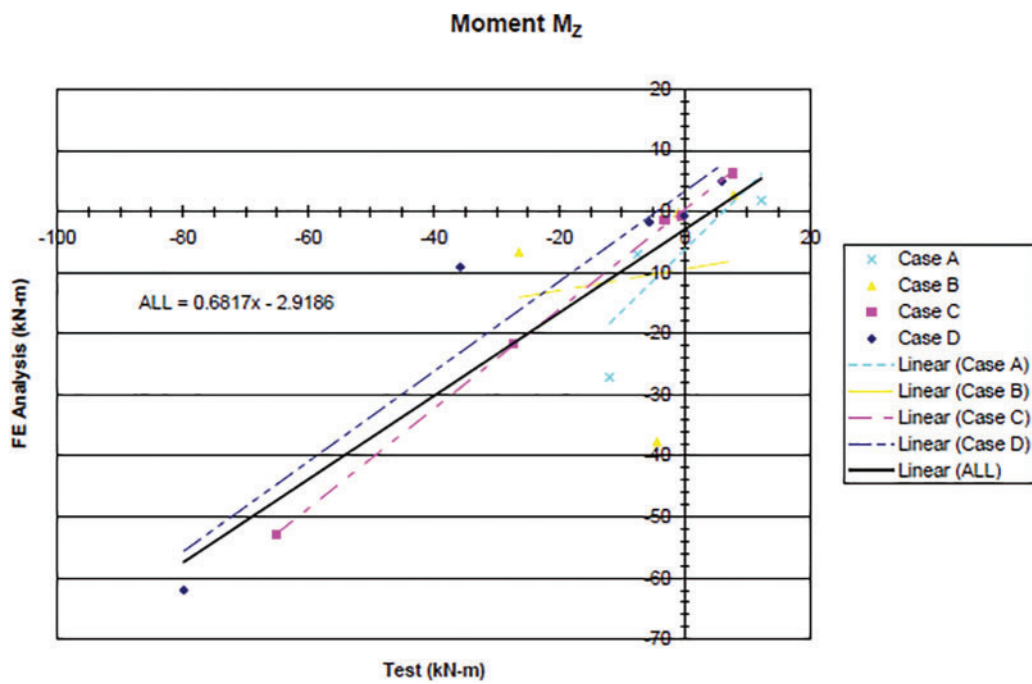


Figure 17. Bending moment (M_z): service live load (FE Analysis) versus load test

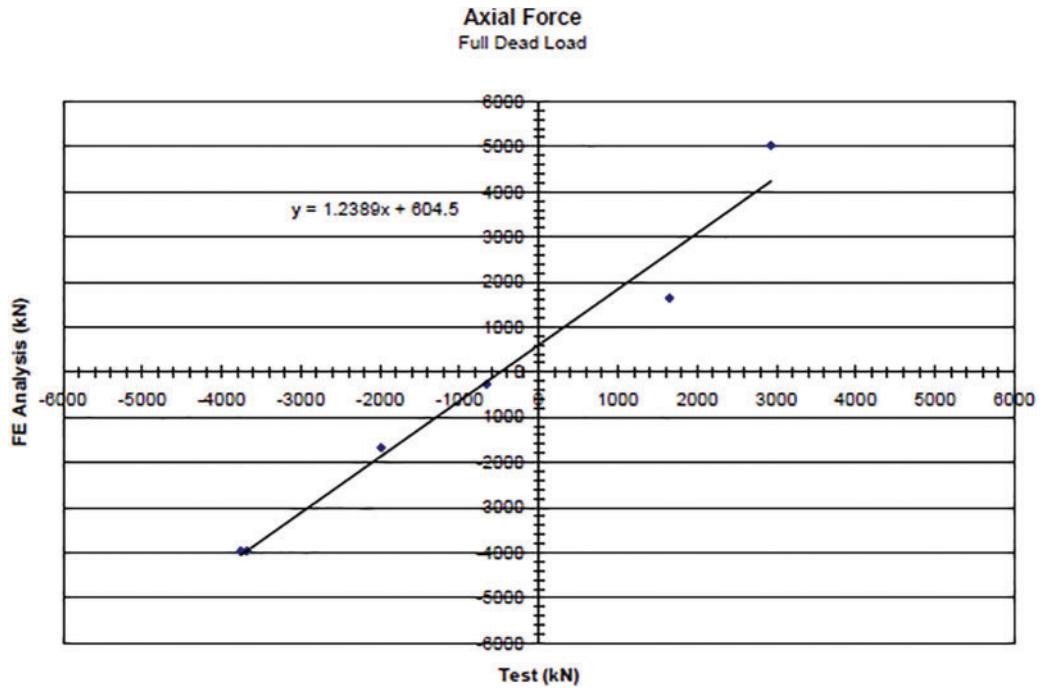


Figure 18. Axial force (F_A): service total dead load (FE Analysis) versus load test

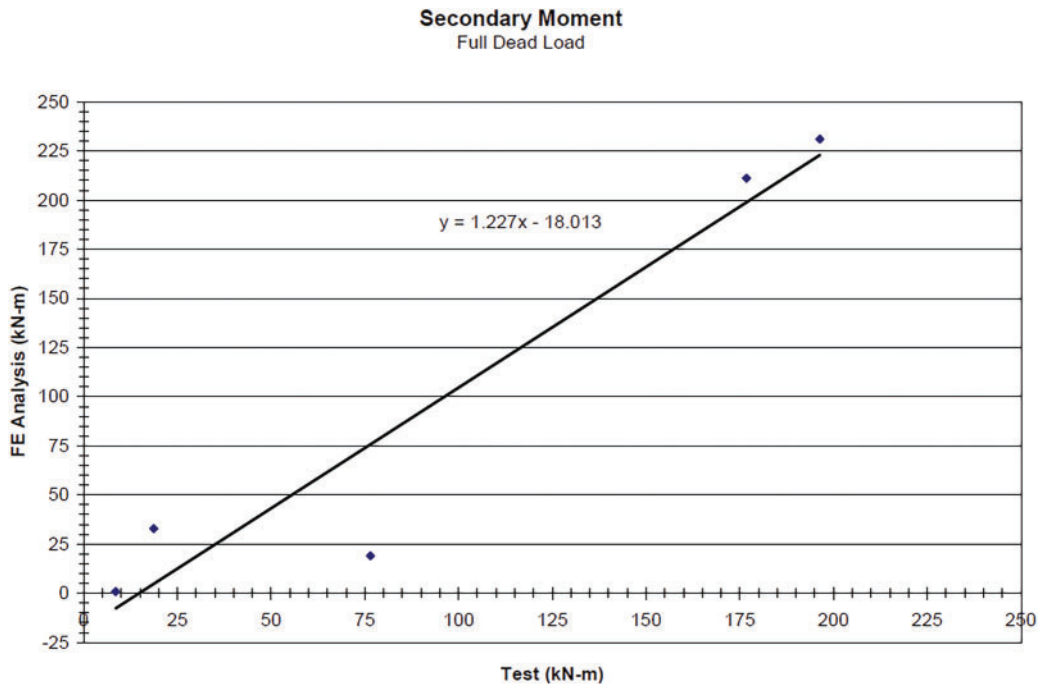


Figure 19. Bending moment (M_z): service dead load (FE Analysis) versus load test

Table 11. Axial forces and moments: design service load vs actual

Member	Service load axial forces and secondary moments											
	Dead load						Live load with impact					
	Axial force (kN)			Secondary moment (kN-m)			Axial force (kN)			Secondary moment (kN-m)		
	FE	Actual	%*	FE	Actual	%*	FE	Actual	%*	FE	Actual	%*
U16-L16	-343	-764	120	1	15	140	-400	-344	14	5	12	140
L16-U17	-2291	-2337	2	38	45	18	-1318	-982	25	28	45	60
L16-L18	-5120	-4621	10	241	211	12	-2652	-1908	28	114	172	50
U17-L18	1931	1071	44	22	32	45	1246	800	35	24	40	66
U16-U17	6423	4696	27	267	232	13	3281	2214	32	224	332	48
Average excluding U16-L16			25				23				30	56

Note: $*\frac{|Actual| - |FE|}{|FE|} \times 100\%$.

Table 12. Checking interaction equations for actual axial forces and moments

Member	Ultimate axial force and moment		Buckling stresses (MPa)		Interaction equations checks			
					Compression + Bending		Tension + Bending	
	P_u (kN)	M_u (kN-m)	F_{cr}	F_e	Equation 10-55*	Equation 10-56*	Equation yield**	Equation LFD-1.8***
U16-L16	-1738	48	308	799	1.019	0.742	-	-
L16-U17	-5169	164	324	1402	0.952	0.775	-	-
L16-L18	-10149	668	464	3067	0.842	0.755	-	-
U17-L18	3131	135	323	1344	-	-	0.7146	0.613
U16-U17	10913	1306	478	11501	-	-	0.832	0.751

Note: ^aAASHTO Standard Specifications. **Checking maximum stress for yielding.

***AASHTO Load Factor Design Specifications.

Table 13. Checking interaction equations for design service loads

Member	Ultimate axial force and moment		Buckling stresses (MPa)		Interaction equations checks			
					Compression + Bending		Tension + Bending	
	P_u (kN)	M_u (kN-m)	F_{cr}	F_e	Equation 10-55*	Equation 10-56*	Equation yield**	Equation LFD-1.8***
U16-L16	-1332	15	308	799	0.547	0.443	-	-
L16-U17	-5957	121	324	1402	0.962	0.810	-	-
L16-L18	-12677	594	464	3067	0.967	0.876	-	-
U17-L18	5313	88	323	1344	-	-	0.894	0.828
U16-U17	9757	971	478	11501	-	-	0.687	0.626

Note: ^aAASHTO Standard Specifications. **Checking maximum stress for yielding.

***AASHTO Load Factor Design Specifications.

Summary and Conclusions

Summary

The results presented in the paper are summarized in Table 11. The actual axial force and secondary moment results in the table were obtained using the linear relationships established in Figs. 18 and 19 for service dead load, and Figs. 16 and 17 for service live load. Table 11 also shows a comparison between the FE analysis and the actual axial force and moment results. Because of the differences between the two result sets noted in the table, it is important to evaluate the design interaction equations for combined stresses using actual axial forces and moments. This evaluation is presented in Table 12. For comparison, the evaluation performed for the design of the members is also included in Table 13. The evaluations in these tables were performed using some of the data included in the tables and the member properties in Tables 2–4.² By comparing the results in Tables 12 and 13, it can be concluded that the actual axial forces and moments satisfied the interaction equations, which confirms the adequacy of the structural design. For the vertical member (U16-L16), the interaction equation is marginally exceeded, which could be attributed to an overestimation of the members' axial forces during the deck pour monitoring.

Conclusions

This and a companion paper discussed the application of load testing techniques for verification of the design of a truss bridge. The bridge is a six-span continuous steel structure about 338 m long and 14.45 m wide. The superstructure is supported by two trusses (an upstream and a downstream) and has a lightweight concrete deck that was built as a composite with the stringers and the top chords of the two trusses. This complicated the design because of the introduced secondary moments in the truss members. The objective of the instrumentation, monitoring, and testing program was to determine actual service load axial forces and secondary moments in the truss members for verification of the bridge design. Vibrating wire gages were mounted on five members of the downstream truss to record strains in those members during the first three deck pours and to collect additional strain data during a load test conducted after the bridge was completed.

The companion paper concluded that the members' actual service dead load axial forces and moments were overestimated by about 20 percent, and service live load axial forces were overestimated by about 30 percent in the design. Regarding moments, it was concluded that service dead load moments were within 25 percent of those used in the design, and service live load moments were underestimated by about 55 percent. The differences between actual and theoretical axial forces and moments for service dead load were attributed to the way the deck pours were accounted for in the design and the possibility of construction loads being present on the deck during the monitoring. The differences between actual and theoretical service live load axial forces

and moments could be explained by the possibility of a discrepancy in estimating actual service live load and the fact that the analysis for service live load in the design was performed assuming a non-composite concrete deck. The adequacy of the structural design was confirmed by checking the AASHTO interaction equations for members under combined stresses using actual axial forces and moments in the bridge members.

This paper employed an approach where limited monitoring coupled with load testing was utilized to investigate actual stresses and load effects at service load levels:

1) It utilized the deck pour monitoring and FE analysis results to estimate axial forces and moments under service total dead load, and

2) It also utilized the load test and FE analysis results to estimate axial forces and moments under design service live load.

3) The paper introduced a pseudo-analytical approach to determine stresses on two normal planes of a member with instrumentation mounted on only one of the member's planes.

4) Based on the three-dimensional FE investigation discussed in the paper, it is recommended that three-dimensional FE models be used for the analysis of structures like Court Street Bridge because of the ability of such models to predict out-of-plane bending, which may result under some loading scenarios. Analyses of dead load and live load data sets, treating the test and FE results as variables, confirmed with very high certainty the statistical significance of the relationships established in the paper between these two variables.

Acknowledgment

The authors acknowledge several past and current NYSDOT staff for their contributions to the project. Instrumentation and data collection were conducted by George Schongar and Harry Greenberg. The STAAD III models used in the analysis were developed by Santiago Lopez and Mary Anne Mariotti. The assistance of Mark Norfolk and Hector Hoyos with the data collection and load testing is particularly acknowledged. The statistical analysis was performed by Dr. Deniz Sandhu. All opinions expressed in this paper are those of the authors and not necessarily of the NYSDOT.

References

- [1] Hag-Elsafi O, Kunin J, Alampalli S. Load testing application for truss bridge design verification: dead load monitoring. Companion paper submitted for journal publication. *Int J Bridge Eng, Manage Res.* 2024. doi:10.32604/ijber.2024.00008.
- [2] Hag-Elsafi O, Kunin J, Alampalli S. *Court Street Bridge Monitoring and Load Testing. Special Report 143, Transportation Research and Development Bureau.* Albany, NY: New York State Department of Transportation; 2006.
- [3] *AASHTO Guide Specifications for Strength Design of Truss Bridges (Load Factor Design).* 1st ed. Washington, D.C:

- American Association of State Highway and Transportation Officials; 1985 including 1986 Interims.
- [4] *New York State Department of Transportation Standard Specifications for Highway Bridges*. New York State Department of Transportation; and provisions in effect as of April 2001.
 - [5] *AASHTO Standard Specifications for Highway Bridges, Including 1997 and 1998 Interim Specifications*. 16th ed. Washington, D.C: American Association of State Highway and Transportation Officials; 1996.
 - [6] *Guide Specifications for Strength Design of Truss Bridges (Load Factor Design)*. Washington, D.C: AASHTO; 1986.
 - [7] Project Design file. *Unpublished, Structures Division*. Albany, NY: New York State Department of Transportation; 2001.